An Example of Temperature Structure Differences in Two Cyclone Systems Derived from the Advanced Microwave Sounder Unit

JOHN A. KNAFF

Cooperative Institute for Research in the Atmosphere, Colorado State University, Fort Collins, Colorado

RAYMOND M. ZEHR

NOAA/NESDIS/RAMM Team, Fort Collins, Colorado

MITCHELL D. GOLDBERG

NOAA/NESDIS/ORA, Washington, D.C.

STANLEY Q. KIDDER

Cooperative Institute for Research in the Atmosphere, Colorado State University, Fort Collins, Colorado

18 August 1999 and 8 March 2000

ABSTRACT

The Advanced Microwave Sounding Unit (AMSU) has better horizontal resolution and vertical temperature sounding abilities than its predecessor, the Microwave Sounding Unit (MSU). Those improved capabilities are demonstrated with observations of two cyclonic weather systems located in the South Pacific Ocean on 1 March 1999. These weather systems appear quite similar in conventional infrared satellite imagery, suggesting that they are comparable in structure and intensity. However, an analysis using temperature retrievals created from the AMSU shows that their vertical thermal structure is quite different.

This is just one example of an application highlighting the improved sounding capabilities available with the AMSU instrument suite. A preliminary look at what the AMSU can provide in data-void regions and a discussion of future plans to create AMSU-based products to better diagnose synoptic-scale weather systems are presented.

1. Introduction

The Advanced Microwave Sounding Unit (AMSU) is the latest operational microwave sounder aboard the National Oceanic and Atmospheric Administration's (NOAA) polar-orbiting satellites. Launched aboard *NOAA-15* on 13 May 1998, it is a considerable advance over its predecessor, the Microwave Sounding Unit (MSU). The instrumentation was designed to make temperature and moisture soundings. The AMSU has more channels and better spatial resolution than previous satellite microwave instruments and is in essence a combination of the best capabilities of all its predecessors.

Three separate instruments compose the AMSU. AMSU-A1 has two channels (1 and 2), AMSU-A2 has 13 channels (3–15), and AMSU-B has five channels (16–20). Collectively AMSU-A1 and -A2 are referred to as AMSU-A, which has the main temperature sounding capabilities. The soundings are determined from channels 3–14, which have frequencies in and near the oxygen microwave absorption band at 57 GHz and have the normalized weighting functions displayed in Fig. 1. The normalized weighting functions of the MSU are shown for comparison. In addition to the increase in number of channels and vertical sounding capabilities, the AMSU also has increased horizontal resolution as shown in Fig. 2.

Two cyclones were observed in the South Pacific Ocean on 1 March 1999 and they had similar appearances in Geostationary Operational Environmental Satellite (GOES) infrared satellite imagery (Fig. 3). AMSU's capabilities to create detailed vertical atmospheric temperature retrievals are demonstrated in this paper with an analysis of those two weather systems. The process of making temperature retrievals is discussed followed by an example of the retrievals applied to the two cyclonic cloud systems. The next section discusses future plans to utilize AMSU for forecasting

Corresponding author address: Dr. John A. Knaff, CIRA/Colorado State University, Foothills Campus, Fort Collins, CO 80523-1375.
E-mail: knaff@cira.colostate.edu

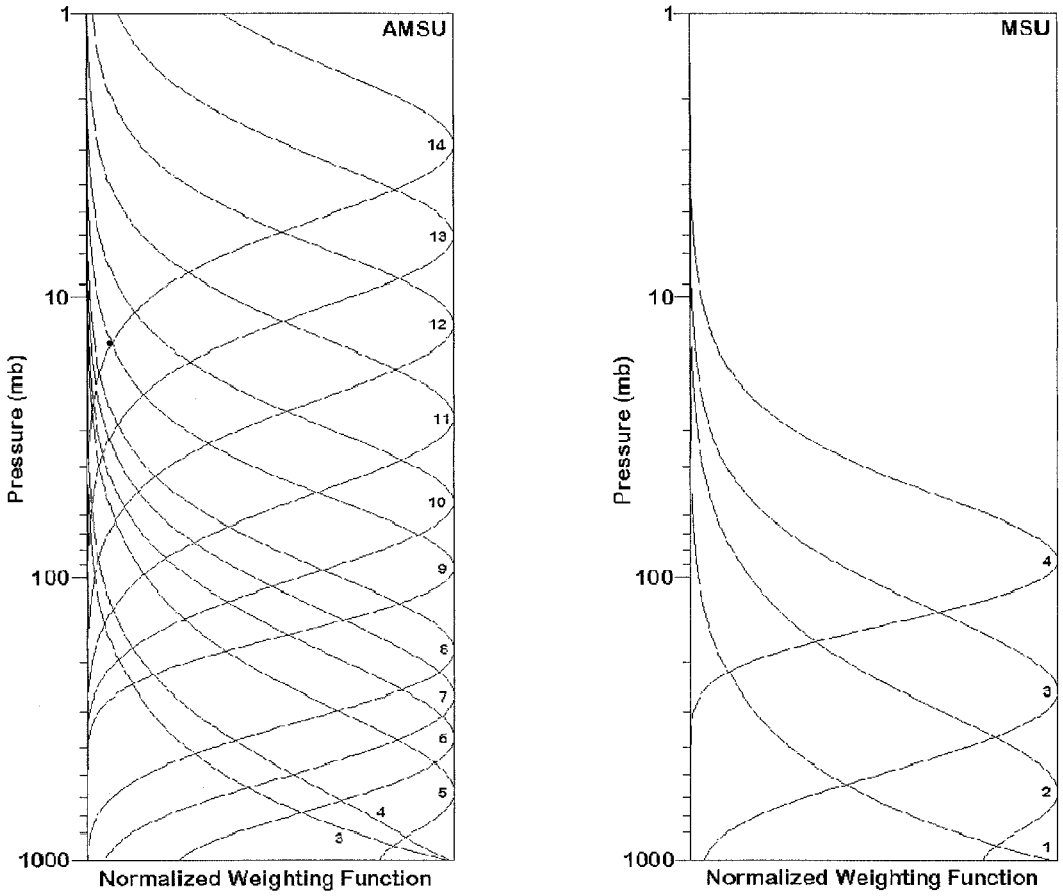

FIG. 1. Comparison of AMSU-A and MSU normalized nadir clear sky weighting functions.

weather systems, followed by a section containing final comments.

2. Temperature retrievals

The temperature retrieval method used for this study has been tailored to climate applications. It utilizes a global linear operator to derive temperature retrievals from a climatological global mean and the input values of the AMSU-A channels (Goldberg 1999). This is in contrast to operational centers that use location-and/or time-specific initial conditions for deriving their final retrieval. This method's results are therefore independent of operational data assimilation and model physics.

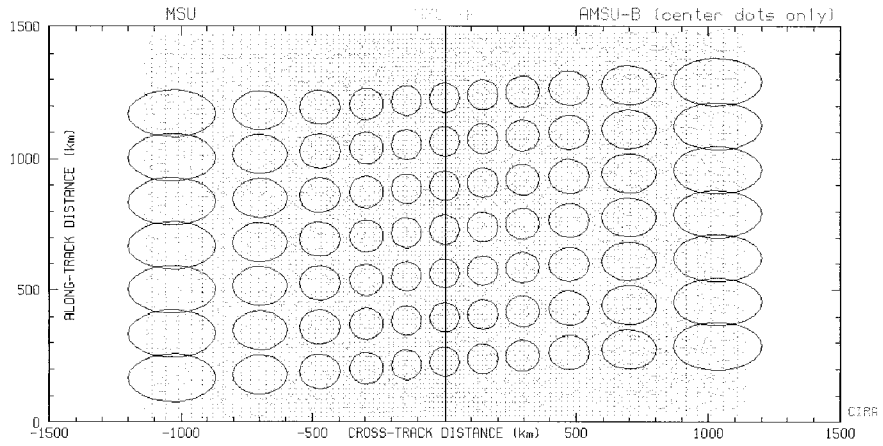

FIG. 2. Comparison of areal coverage or footprint size of the MSU and the AMSU-A.

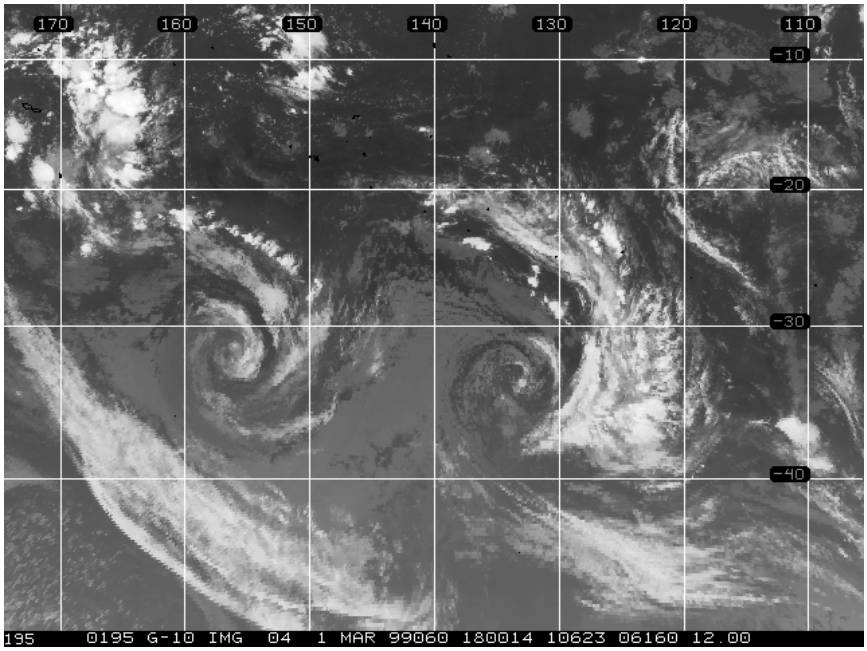

FIG. 3. Infrared satellite picture at 1800 UTC on 1 Mar 1999 of two South Pacific cyclone systems that appear to be quite similar. The projection is Mercator and the resolution is 12 km.

Unlike infrared observations, the microwave sounder observations have a linear relationship between temperature and the Planck radiance. This means that a climatological first guess is all that is needed to compute a good temperature profile. For monitoring temperature trends, this type of processing is advantageous. Because this method does not rely upon a model first-guess temperature field or other ancillary data, the retrievals are useful in data-sparse regions.

The processing of AMSU-A data to retrieve atmospheric temperatures includes several steps. First, two corrections must be made. The first correction accounts for antenna sidelobes and is described by Mo (1999). The algorithm creates brightness temperatures from the raw antenna temperatures. A second correction adjusts these brightness temperatures to look like nadir observations, accounting for the 30 different view angles. This limb adjustment procedure is based on the work of Wark (1993) and 31 days of data (1–31 Jul 1998) were used to develop the method.

From the limb-adjusted brightness temperatures, atmospheric temperature is retrieved at 40 pressure levels between 1000 and 0.1 hPa using the linear retrieval operator (LRO). The LRO is derived from collocated rawindsonde data, for pressure levels below 10 hPa, and from temperature profiles of 6000 rocketsondes, above 10 hPa. A radiative transfer algorithm was used to compute AMSU brightness temperatures from the observed profiles. The LRO, which relates AMSU brightness temperature to atmospheric temperature, was then computed. It is important to note that the channel combination used for each level is not the same. In addition, temperature retrievals use channels that reduce the occurrence of contamination from terrain. From 700 to 115 hPa, channels lower than channel 6 are not used to reduce the occurrence of contamination from precipitation. A global set of coefficients is used from 700 hPa and above, whereas in the layer 780–1000 hPa, there are two sets of coefficients, one for ocean, the other for land surfaces.

The final step is a bias correction. This adjustment is needed to account for the bias between actual brightness temperatures and those computed using the radiative transfer algorithm. Collocated rawinsonde and AMSU data were used to compute the bias. This bias is then applied in the retrieval step. The resulting standard deviation errors of the retrieved temperature are less than 2°C for all sky conditions during both day and night (Goldberg 1999). [See http://orbit-net.nesdis.noaa.gov/crad/st/amsuclimate/val.html for Jul 1998 validation and Goldberg (1999) for the Nov–Dec 1998 validation.]

Microwave remote sensing is strongly influenced by the contamination from precipitation, particularly heavy rainfall. In regions of heavy rainfall, temperature retrievals are erroneously cold due to this contamination. This contamination is particularly pronounced in the lower-tropospheric temperature retrievals, and in some cases it can affect temperature retrievals even at higher levels. Efforts are under way to correct temperature retrievals in the whole troposphere when there is heavy precipitation. At present, however, we confine our example to the upper and midlevels of the troposphere and

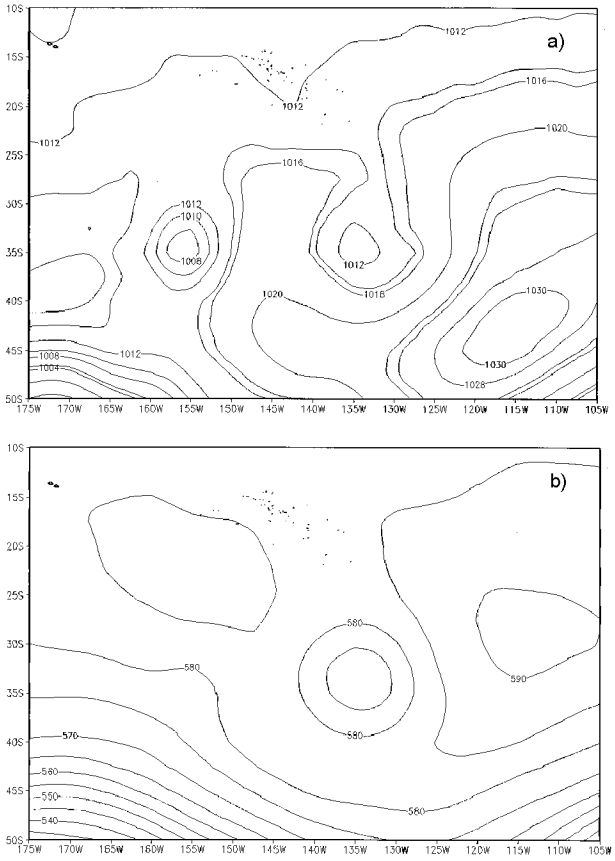

FIG. 4. (a) Surface pressure and (b) 500-hPa analyses valid 0000 UTC 2 Mar.

lower stratosphere where this type of contamination is less likely to occur.

3. Example: Observations and discussion

Two distinctive cyclonic cloud patterns are seen in Fig. 3, one centered around 32°S, 157°W and another at 33°S, 133°W. Qualitatively they appear quite similar, suggesting they may be comparable with regard to structure and intensity. The surface pressure analysis valid at 0000 UTC on 2 March shows that both systems had surface circulations and central pressures less than 1012 hPa, as shown in Fig. 4a. However, an analysis of the *NOAA-15* AMSU temperature retrievals valid near 1800 UTC on 1 March reveals that their vertical thermal structures were quite different, as shown in Figs. 5–7 at 570, 350, and 250 hPa, respectively. Figure 4b shows the corresponding 500-hPa analysis. The center of the eastern system was colder than its surroundings in the middle troposphere (570 hPa), while the western system had a weak midlevel warm core, as shown in Fig. 5. At 350 hPa (Fig. 6), the same temperature pattern is analyzed, showing the cold core structure was a bit weaker with the eastern system. In the upper troposphere, as shown by the 250 hPa analysis in Fig. 7, the western

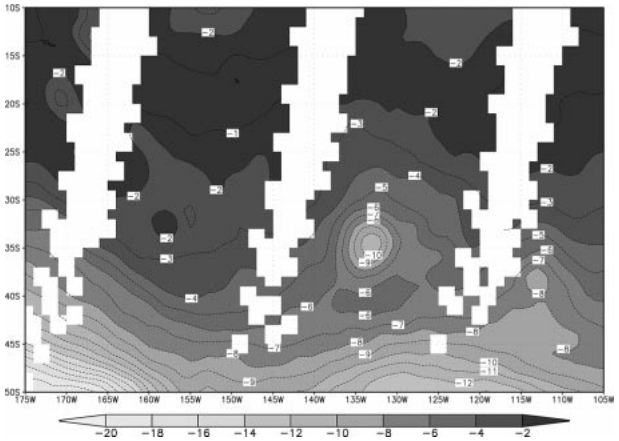

FIG. 5. The 570-hPa AMSU temperature retrieval analysis (°C) for the same area as shown in Fig. 3. The individual satellite swaths are roughly at 1750 and 1520 UTC on 1 Mar for the western cyclone and eastern cyclone, respectively.

system still showed a warm core, while the eastern system at this level had a very prominent warm anomaly.

These AMSU observations compare well with the distinctly different histories of the two cyclones. The western storm is a weakening tropical cyclone tracking to the south over colder water. It originated on 25 February near the Cook Islands around 15°S, 165°W. The system was upgraded to Tropical Cyclone Gita at 0000 UTC on 27 February. It then attained a maximum intensity of 23 m s^{-1} (45 kt), (10-min average surface wind speed), on 28 February at 0600 UTC. This is based on the advisory issued by the Wellington, New Zealand, Regional Specialized Meteorological Center. Atypical of most tropical cyclones in this region, Gita was not steered to the east and south by a passing midlatitude trough. In a relatively weak steering environment with gradually cooling SSTs, the cyclone spun down slowly, continuing to generate some convection near the center until 2 March. This probably allowed the preexisting warm core temperature structure to remain intact until

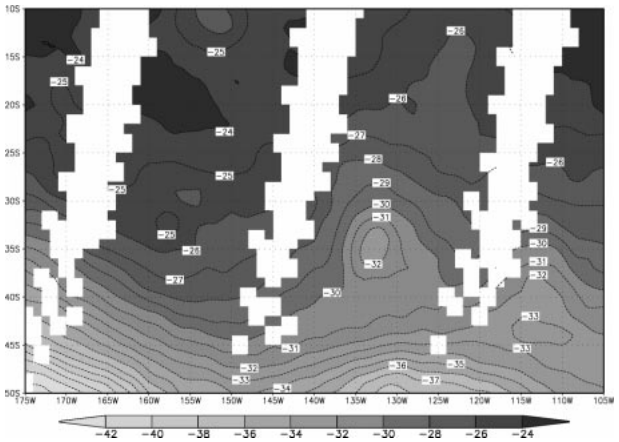

FIG. 6. Same as in Fig. 2 except at 350 hPa.

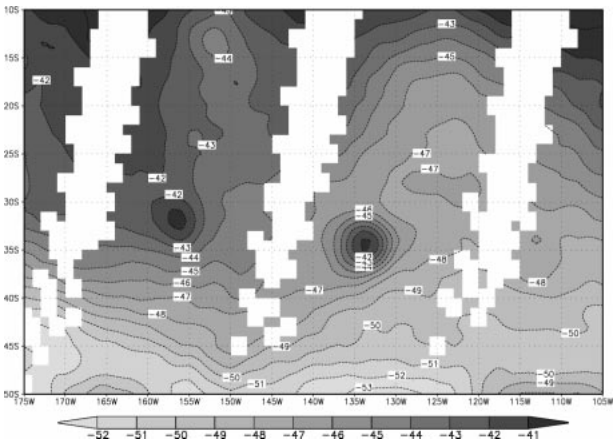

FIG. 7. Same as in Fig 3 except at 250 hPa.

viewed by AMSU as seen in the vertical cross section shown in Fig. 8. In addition to the general warm core appearance, there are also signs of liquid water contamination in the retrieval cross section below 500 hPa as indicated by cold temperature anomalies and temperature asymmetries in the middle levels.

Tropical cyclones typically have a deep tropospheric layer of warm anomalies relative to their surroundings, with the warmest anomalies near 300–250 hPa and maximum wind speeds near the surface (Hawkins and Rubsam 1968; Hawkins and Imbembo 1976; Frank 1977). Microwave instruments can measure this upper-level warm core quite well. In the past, several methods have been developed using other microwave satellite data to utilize this measurement to make estimates of tropical cyclone intensity and surface pressure fields (Kidder et al. 1978, 1980; Velden and Smith 1983; Velden 1989; Velden et al. 1991). The improved resolution of the AMSU observations has caused a resurgence of interest in these types of measurements (Kidder et al. 2000).

The eastern cyclone is a subtropical cold low, which never developed tropical cyclone characteristics. It was tracked for several days in the GOES water vapor images and in 500-hPa height fields. As often is the case in the North Atlantic and North Pacific, this subtropical system began as a middle- and upper-level low center that had been cut off from the main midlatitude jet. The cutoff low first appeared in the 500-hPa analysis at 0000 UTC on 28 February. At this time, there was only a weak surface pressure trough extending from the Tropics. As time progressed, the cutoff low began to work its way to the surface forming a closed surface circulation directly under the midlevel circulation at 0000 UTC on 1 March. The system continued to become better organized with occasional convection near its center and was accompanied by a more symmetric circulation and lower pressure through 0000 UTC on 2 March (see Fig 4b). At the time of the AMSU analysis, it was moving slowly to the north after tracking to the east along 40°S and had surface pressures less than 1012

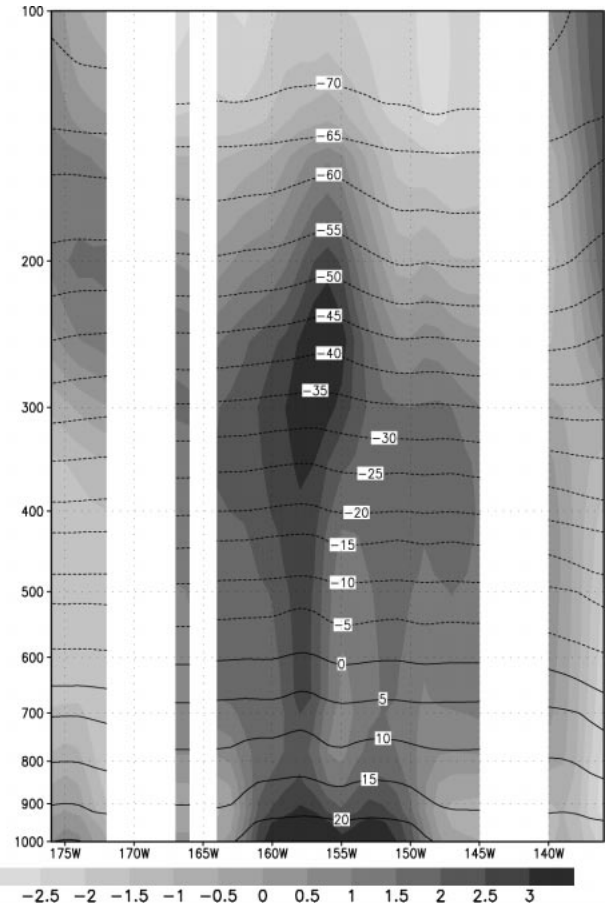

FIG. 8. Longitude vs log$p$ cross section of temperature in °C (contours) and temperature anomalies from the zonal mean (shaded) of Tropical Storm Gita at approximately 1750 UTC 1 Mar.

hPa. The system had the clear structure of a strong, vertically stacked, cutoff, low pressure system as shown in Fig. 9.

Subtropical lows have a deep tropospheric layer with cold anomalies relative to their surrounding area, topped by large positive temperature anomalies in the 300–150-hPa layer. This warm core may be either above the tropopause or above a secondary tropopause at a lower level (Simpson 1952; Erickson 1967). This temperature profile results in maximum wind speeds in the upper or midtroposphere below the level of maximum warm anomaly. These are hybrid systems that are cold core to start, usually originating from a midlatitude cutoff low. With time, however, these systems develop convection near their centers and begin to create a warm core in the lower levels in addition to their cold core. These subtropical cold lows are similar to, but stronger and deeper than, the more common summertime cold lows that occur in all ocean basins, and are sometimes referred to as tropical upper-tropospheric trough cells (Sadler 1976; Kelley and Mock 1982; Fitzpatrick et al. 1995).

Comparing the cross sections of temperature between

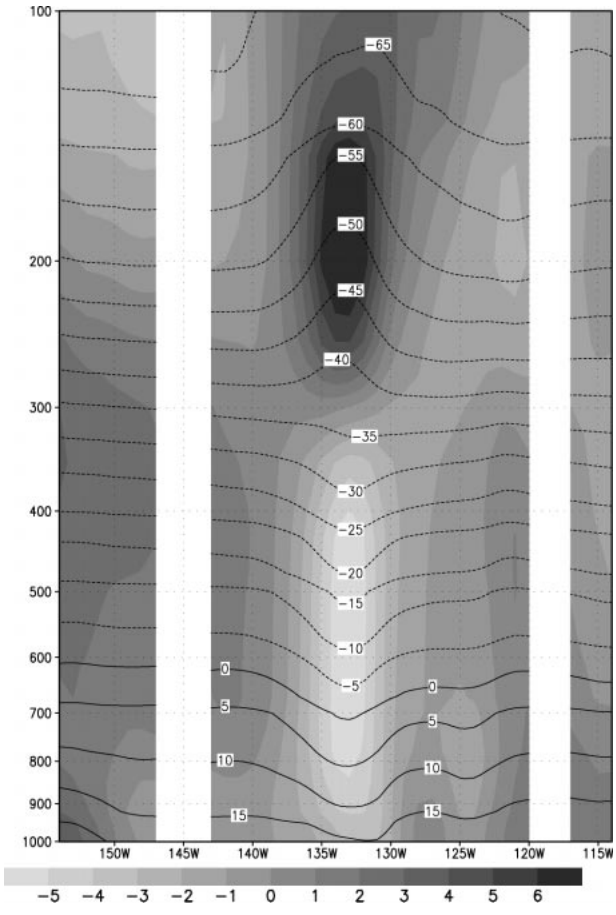

FIG. 9. Longitude vs log*p* cross section of temperature in °C (contours) and temperature anomalies from the zonal mean (shaded) of the subtropical low approximately 1520 UTC 1 Mar.

the two systems, there are clear differences. At the times these cross sections were produced, only small amounts of deep convection were associated with either system, and the AMSU-derived temperature profiles likely had little precipitation-induced contamination. It is clear that the eastern system is a cold core low that is cut off from the midlatitude jet and that the western system is a warm core low of a weak tropical cyclone.

In contrast to the systems shown here, midlatitude (extratropical) cyclones have a more complex structure. These cyclones are strongly influenced by the strength and positioning of upper-level baroclinic waves and have a structure in which the axis of maximum cyclonic vorticity is often strongly tilted with height (Bluestein 1993). This axis extends from near the low-level cold anomaly to the stratospheric warm anomaly that corresponds with the lowest tropopause and the coldest upper-tropospheric air. Although these systems are not discussed here, there is little doubt that these systems too can be better monitored in data-sparse regions using the sounding capabilities of the AMSU.

The vertical resolution of the AMSU temperature profile is a great improvement over the MSU. This temperature information can be used for many potential applications beyond the qualitative interpretation offered in this paper. Work is under way to utilize more quantitative temperature analyses to augment other readily available information that will aid forecasters. The next section will discuss plans to utilize the AMSU data.

4. Utilization of AMSU

The vertical and horizontal resolution improvements of the AMSU, along with recent improvements in computing and information sharing capabilities, make possible several near-real-time applications of AMSU data. Some applications have been suggested in the past and will be improved with the new capabilities of AMSU, while other applications are unique to the information available from the AMSU.

One application of microwave sounders is monitoring synoptic weather systems, both tropical and nontropical. With tropical cyclones, the monitoring of the size and strength of the upper-level warm core, which is related to the surface wind speed, and the central pressures of the tropical cyclones is one clear application that would be improved by the use of AMSU. Past studies of this type include Kidder et al. (1978, 1980), Velden and Smith (1983), Velden (1989), and Velden et al. (1991), but they have always been limited by the resolution of past microwave sounding instruments.

AMSU's resolution is also somewhat of an issue because the horizontal resolution is still far too coarse to observe the eyewall region of the tropical cyclone. However, the better resolution both in the vertical and in the horizontal can be used to better isolate the height, strength, and size of the warm anomaly. The hope is that the AMSU will produce an intensity estimate that is independent of the Dvorak (1984) intensity estimate method where aircraft reconnaissance is not available. However, a developmental dataset for such a method must be first collected where ground truth (aircraft) is available.

In addition to the monitoring of the warm core anomalies, the increased resolution allows for the more precise calculation of height and pressure gradients from temperature profiles and analysis fields (model analysis). This can be accomplished by assuming hydrostatic balance and integrating inward and downward toward the cyclone center using the surface pressure along the edges of the AMSU domain and the surface temperature at the lowest level from model analyses as anchors. Using the height fields and assuming gradient balance, wind fields can be computed. Presently this type of analysis is being performed in near–real time at NOAA's Cooperative Institute for Research in the Atmosphere. This work is being conducted and supervised by M. DeMaria and involves all of the authors of this paper in some way. Details of the calculations are discussed in Kidder et al. (2000). At present, the wind field is being calculated for an azimuthally averaged height

field, but in the future, the three-dimensional wind field will be produced and displayed. (To see examples of this work and real-time storm coverage go to http://www.cira.colostate.edu/ramm/tropic/amsustrm.asp.)

The derivation of the wind field provides information, often unavailable to the forecaster, concerning radii of significant winds. The radii of gale and hurricane force winds are forecast requirements that are difficult to estimate without reconnaissance data. To make this problem more difficult, the radii of significant winds are not be well related to the maximum wind speed or to minimum sea level pressure (Weatherford and Gray 1988). Here again work is under way and a developmental dataset is being collected, but as for intensity estimates, ground truth measurements of the winds are needed.

As alluded to earlier, one of the central problems with the AMSU-derived temperature profiles is the effect of heavy rainfall. With many examples of tropical cyclones, this contamination is very clear. There are efforts under way to address these problems. The present AMSU tropical cyclone products use a simple correction. It has been found that in the middle and upper layers, temperature contamination (cooling) is to a first approximation a linear function of cloud liquid water (clw) path, which is calculated using AMSU channels 1 and 2. Using footprints within the AMSU domain that have no rainfall (clw $<$ 0.03 mm) to construct a level-mean temperature for the area around a hurricane, a linear regression is performed on the temperature anomalies, based on this level mean and the clw. The regression coefficient or slope is then used to make a first-order correction to the observed temperature at each level. This simple correction is temporary while other more elegant methods are being explored.

The AMSU also has many potential applications to aid the midlatitude weather forecaster. MSU observations have been used with several techniques for analysis of extratropical cyclones. One technique uses MSU channel 3 (MSU3), which senses at 54.96 GHz, to observe upper-tropospheric/lower-stratospheric warming on synoptic length scales. Variations of MSU3 are related to the strength of the synoptic-scale cyclones, and trends of MSU3 have been demonstrated to be useful in determining changes in cyclone intensity (Velden 1992). It has been shown that upper-level thermal anomalies are significantly related to 200-hPa temperatures and to 100–400-hPa thickness, but even more important, they are reflected downward to 500 hPa on synoptic scales as shown in Hirschberg et al. (1997).

Information from the MSU has even been used to estimate vorticity and vertical motion. In this formulation, MSU3 is used to estimate geostrophic vorticity and the gradient of the linear combination of MSU3 and MSU2 is used to diagnose the midtropospheric thermal wind. Vertical motion is then estimated from the advection of the geostrophic vorticity by the thermal wind (see Spencer et al. 1995 for details). This clever method may not be required given the improved vertical sounding capabilities of AMSU.

As mentioned above, using a model analysis for surface temperatures and surface pressures around the domain, height, and pressure fields can be constructed using AMSU temperature profiles. In the extratropics, there are added advantages with AMSU; contamination by rain is not as severe, and the temporal coverage is complete without the spatial gaps between data that occurs near the equator. Using AMSU-derived height fields, gradient winds can be calculated using the methods described in Kasahara (1982). From the wind and temperature fields a much more detailed diagnosis of vorticity, divergence, and vertical motion can be calculated. These can then be compared with other analysis from various models and data assimilation packages. At present, this work is nearing completion. The domain for this analysis will be centered in the North Pacific Ocean downstream of the U.S. west coast. It is hoped that this information will aid the forecaster in better diagnosing incoming weather systems.

5. Final comments

The new microwave sounder on the NOAA polar-orbiting operational satellites (AMSU) is a great improvement over its predecessor, having greater horizontal as well as vertical resolution. A simple example of some of its vertical profiling capabilities is shown here. This example demonstrates AMSU's ability to determine detailed vertical structures of weather systems. In the future, AMSU temperature retrievals will help to document the thermal structure of all weather systems. This information will be particularly useful for analyzing systems occurring in oceanic, tropical, and polar regions where conventional data are scarce.

In addition to thermal structures, dynamical information can be derived allowing a better view of weather systems in data-sparse regions. To improve AMSU applications to the analysis of weather systems, methods must be devised to deal with liquid water contamination of the microwave signal in the lower troposphere. The contamination is particularly prevalent in the Tropics where liquid water exists to higher levels of the atmosphere. In the meantime, the future looks bright for the development of many products to help forecasters diagnose weather system when conventional data are unavailable or unreliable. Dynamical and thermal fields for both tropical and extratropical systems can be derived utilizing the AMSU. Specific products include estimates of tropical cyclone intensities and radii of significant winds and wind fields in the data-sparse oceanic regions. In addition, detailed surface wind analyses are produced for tropical and midlatitude cyclones.

Acknowledgments. This research is supported by NOAA Grant NA67RJ0152. The first author is supported by the Severe Weather Prediction Initiative. We

would like to thank the anonymous reviewers for their helpful comments and acknowledge that the sea level pressure and 500-hPa map displayed in Fig. 4 came for the NOAA Climate Diagnostic Center. Special thanks to Mark DeMaria, whose ideas make up much of the upcoming utilization of AMSU data discussed in this paper.

REFERENCES

Bluestein, H. B., 1993: *Synoptic-Dynamic Meteorology in Midlatitudes.* Vol. II, *Observations and Theory of Weather Systems.* Oxford University Press, 594 pp.

Dvorak, V. F., 1984: Tropical cyclone intensity analysis using satellite data. NOAA Tech. Rep. NESDIS 11, 47 pp. [Available from NOAA/NESDIS, 5200 Auth Rd., Washington, DC 20233.]

Erickson, C. O., 1967: Some aspects of the development of Hurricane Dorothy. *Mon. Wea. Rev.,* **95,** 121–130.

Fitzpatrick, P. J., J. A. Knaff, C. W. Landsea, and S. V. Finley, 1995: Documentation of a systematic bias in the aviation model's forecast of the Atlantic tropical upper tropospheric trough: Implications for tropical cyclone forecasting. *Wea. Forecasting,* **10,** 433–446.

Frank, W. M., 1977: The structure and energetics of the tropical cyclone I. Storm structure. *Mon. Wea. Rev.,* **105,** 1119–1135.

Goldberg, M. D., 1999: Generation of retrieval products from AMSU-A: Methodology and validation. *Proc. 10th Int. TOVS Study Conf.* Boulder, CO.

Hirschberg, P. A., M. C. Parke, C. H. Wash, M. Mickelinc, R. W. Spencer, and E. Thaler, 1997: The usefulness of MSU3 analyses as a forecasting aid: A statistical study. *Wea. Forecasting,* **12,** 324–346.

Hawkins, H. F., and D. T. Rubsam, 1968: Hurricane Hilda, 1964, II. Structure and budgets of the hurricane on October 1 1964. *Mon. Wea. Rev.,* **96,** 617–636.

——, and S. M. Imbembo, 1976: The structure of a small, intense hurricane—Inez 1966. *Mon. Wea. Rev.,* **104,** 418–442.

Kasahara, A., 1982: Significance of non-elliptic regions in balanced flows of the tropical atmosphere. *Mon. Wea. Rev.,* **110,** 1956–1967.

Kelley, W. E., Jr., and D. R. Mock, 1982: A diagnostic study of upper tropospheric cold lows over the western North Pacific. *Mon. Wea. Rev.,* **110,** 471–480.

Kidder, S. Q., W. M. Gray, and T. H. Vonder Haar, 1978: Estimating tropical cyclone pressure and outer winds from satellite microwave data. *Mon. Wea. Rev.,* **106,** 1458–1464.

——, ——, and ——, 1980: Tropical cyclone outer surface winds derived from satellite microwave sounder data. *Mon. Wea. Rev.,* **108,** 144–152.

——, M. D. Goldberg, R. M. Zehr, M. DeMaria, J. F. W. Purdom, C. S. Velden, N. C. Grody, and S. J. Kusselson, 2000: Satellite analysis of tropical cyclones using the Advanced Microwave Sounding Unit (AMSU). *Bull. Amer. Meteor. Soc.,* **81,** 1241–1259.

Mo, T., 1999: AMSU-A antenna pattern corrections. *IEEE Trans. Geosci. Remote Sens.,* **37,** 103–112.

Sadler, J. C., 1976: A role of the tropical upper tropospheric trough in early season typhoon development. *Mon. Wea. Rev.,* **104,** 1266–1278.

Simpson, R. H., 1952: Evolution of the Kona storm, a subtropical cyclone. *J. Meteor.,* **9,** 24–35.

Spencer, R. W., W. M. Lapenta, and F. R. Robertson, 1995: Vorticity and vertical motions diagnosed from satellite deep-layer temperatures. *Mon. Wea. Rev.,* **123,** 1800–1810.

Velden, C. S., 1989: Observational analyses of North Atlantic tropical cyclones from NOAA polar-orbiting satellite microwave data. *J. Appl. Meteor.,* **28,** 59–70.

——, 1992: Satellite-based microwave observations of tropopause-level thermal anomalies: Qualitative applications in extratropical cyclone events. *Wea. Forecasting,* **7,** 669–682.

——, and W. L. Smith, 1983: Monitoring tropical cyclone evolution with NOAA satellite microwave observations. *J. Climate Appl. Meteor.,* **22,** 714–724.

——, B. M. Goodman, and R. T. Merill, 1991: Western North Pacific tropical cyclone intensity estimation from NOAA polar-orbiting satellite microwave data. *Mon. Wea. Rev.,* **119,** 159–168.

Wark, D. Q., 1993: Adjustment of TIROS Operational Vertical Sounder data to a vertical view. NOAA Tech. Rep. NESDIS 64, Washington, DC, 36 pp. [Available from NOAA/NESDIS, 5200 Auth Rd., Washington, DC 20233.]

Weatherford, C. L., and W. M. Gray, 1988: Typhoon structure as revealed by aircraft reconnaissance. Part II: Structural variability. *Mon. Wea. Rev.,* **116,** 1044–1056.